Cancer Cell
Article

Hepatic RIG-I Predicts Survival and Interferon-α Therapeutic Response in Hepatocellular Carcinoma

Jin Hou,[1,2,12] Ye Zhou,[1,12] Yuanyuan Zheng,[1,12] Jia Fan,[3] Weiping Zhou,[4] Irene O.L. Ng,[5] Huichuan Sun,[3] Lunxiu Qin,[3] Shuangjian Qiu,[3] Joyce M.F. Lee,[5] Chung-Mau Lo,[5] Kwan Man,[5] Yuan Yang,[4] Yun Yang,[4] Yingyun Yang,[2] Qian Zhang,[1,2] Xuhui Zhu,[1] Nan Li,[1] Zhengxin Wang,[6] Guoshan Ding,[6] Shi-Mei Zhuang,[7] Limin Zheng,[7] Xiaoling Luo,[8] Yuan Xie,[8] Anmin Liang,[8] Zhugang Wang,[9] Ming Zhang,[10] Qiang Xia,[10] Tingbo Liang,[11] Yizhi Yu,[1] and Xuetao Cao[1,2,*]
[1]National Key Laboratory of Medical Immunology and Institute of Immunology, Second Military Medical University, Shanghai 200433, China
[2]National Key Laboratory of Medical Molecular Biology and Department of Immunology, Chinese Academy of Medical Sciences, Beijing 100005, China
[3]Department of Hepatic Surgery, Liver Cancer Institute and Zhongshan Hospital, Institutes of Biomedical Science, Fudan University, Shanghai 200032, China
[4]Third Department of Hepatic Surgery, Eastern Hepatobiliary Surgery Hospital, Shanghai 200438, China
[5]Departments of Pathology and Surgery, State Key Laboratory for Liver Research, University of Hong Kong, Hong Kong 999077, China
[6]Department of Organ Transplantation, Shanghai Changzheng Hospital, Shanghai 200003, China
[7]Key Laboratory of Gene Engineering of the Ministry of Education, School of Life Sciences, Sun Yat-sen University, Guangzhou 510275, China
[8]Department of Surgery, Affiliated Tumor Hospital, Guangxi Medical University, Nanning 530021, China
[9]Department of Medical Genetics, Shanghai Jiao Tong University School of Medicine, Shanghai 200025, China
[10]Department of Transplantation and Hepatic Surgery, Renji Hospital, Shanghai Jiaotong University School of Medicine, Shanghai 200127, China
[11]Department of Surgery, Second Affiliated Hospital, Zhejiang University School of Medicine, Hangzhou 310009, China
[12]These authors contributed equally to this work
*Correspondence: caoxt@immunol.org
http://dx.doi.org/10.1016/j.ccr.2013.11.011

SUMMARY

In hepatocellular carcinoma (HCC), biomarkers for prediction of prognosis and response to immunotherapy such as interferon-α (IFN-α) would be very useful in the clinic. We found that expression of retinoic acid-inducible gene-I (*RIG-I*), an IFN-stimulated gene, was significantly downregulated in human HCC tissues. Patients with low RIG-I expression had shorter survival and poorer response to IFN-α therapy, suggesting that RIG-I is a useful prognosis and IFN-α response predictor for HCC patients. Mechanistically, RIG-I enhances IFN-α response by amplifying IFN-α effector signaling via strengthening STAT1 activation. Furthermore, we found that *RIG-I* deficiency promotes HCC carcinogenesis and that hepatic RIG-I expression is lower in men than in women. RIG-I may therefore be a tumor suppressor in HCC and contribute to HCC gender disparity.

INTRODUCTION

Hepatocellular carcinoma (HCC) is one of the most common cancers worldwide and is among the leading causes of cancer-related death, especially in China (El-Serag, 2011). Until now, surgery has remained the most effective treatment with curative potential, but only 30%–40% of HCC patients are diagnosed at early stages and amenable to potentially curative surgical therapy. However, patients who have undergone radical tumor resection have a high rate of relapse, and a 5 year survival rate is only about 60% in well-selected patients (Llovet et al., 2003). Systemic and targeted therapies, such as transcatheter arterial chemoembolization, sorafenib, and interferon-alpha (IFN-α), may provide clinical benefit in prolonging patients'

Significance

Analysis of interferon-stimulated gene (ISG) expression in hepatocellular carcinoma (HCC) revealed that retinoic acid-inducible gene-I (RIG-I) expression is significantly downregulated in HCC. RIG-I was also found to promote interferon-α (IFN-α) effector signaling and therapeutic response in HCC. Together with clinical data that patients whose tumors exhibited low RIG-I expression had shorter survival and poorer response to IFN-α therapy, we propose that RIG-I expression in HCC tissue may be useful as an HCC prognosis marker and in identifying good responders to IFN-α therapy. Furthermore, RIG-I may contribute to HCC gender disparity, as its expression in liver tissues is significantly lower in men than in women. *RIG-I* deficiency also promotes HCC carcinogenesis in mice.

survival, but the difficulty in identifying patients who might respond well often makes these targeted adjuvant therapies less effective (Finn, 2008; Melief, 2008; Zou, 2005; Sun et al., 2006; Lo et al., 2007; Clavien, 2007; Llovet et al., 2008). For IFN-α, a promising but incompletely understood anticancer agent, clinical trials have demonstrated benefit in both hematological and solid tumors, although the effectiveness is somewhat modest in HCC (Sun et al., 2006; Lo et al., 2007; Clavien, 2007). IFN-α therapy has been suggested to be effective in a subgroup of HCC patients, and it has been suggested that patients with single-nodule tumor and ablation therapy or low miR-26a expression in HCC tend to respond better to adjuvant IFN-α treatment (Ji et al., 2009; Shen et al., 2010). Thus, identification of molecular biomarkers that can identify HCC patients sensitive to IFN-α therapy would be very helpful in the clinic.

IFN-α has various biological properties, including antiviral response, immune modulation, and antiproliferative activity (Taniguchi and Takaoka, 2001). It has therefore been widely used for the treatment of viral infections and cancer. The binding of IFN-α to its cell-surface receptors activates the downstream Janus kinase (JAK) signal transducer and the activator of transcription (STAT) signaling cascade, which then induces the transcription of a set of genes, namely IFN-stimulated genes (ISGs). Currently, about 300 ISGs have been identified through oligonucleotide microarray studies, and these ISGs are responsible for diverse biological functions of IFN-α, including its antitumor activity (Platanias, 2005; Chawla-Sarkar et al., 2003). The functions of ISGs in the regulation of infection and cancer, including HCC, and how they might modulate responses to IFN-α therapy are still not well understood.

RIG-I is well established to be one of the critical sensors for host recognition of RNA virus infection and subsequent induction of type I IFN. It contains a C-terminal helicase domain to recognize cytoplasmic viral RNA such as that of influenza virus and two N-terminal tandem caspase-recruiting domains (CARDs) to activate downstream signaling and induce type I IFN production (Takeuchi and Akira, 2010; Luo et al., 2011; Kowalinski et al., 2011; Jiang et al., 2011a; Chen et al., 2013b). As one of the ISGs, RIG-I expression is markedly induced upon IFN-α stimulation, but the roles of RIG-I in IFN-α responses are still unknown. Here we focused on the roles of RIG-I in the control of HCC carcinogenesis and progression, especially its role and the underlying mechanism in IFN-α therapeutic response of HCC patients.

HCC occurs mainly in men, one of the key and most interesting features of HCC carcinogenesis (El-Serag and Rudolph, 2007). In a diethylnitrosamine (DEN)-induced HCC mouse model, it was demonstrated that male mice were more susceptible as a result of the enhanced production of proinflammatory cytokines, such as interleukin-6 (IL-6) (Naugler et al., 2007; Park et al., 2010). Other factors, such as sex hormones, menstruation, pregnancy, oral contraceptive usage, and endocrinology disorders have also been proposed to be associated with HCC carcinogenesis (Buch et al., 2008; Ruggieri et al., 2010; Vana et al., 1977). Furthermore, female HCC patients tend to have longer survival times than men, suggesting that differentially expressed molecules between genders or gender-related factors might be associated with both HCC carcinogenesis and prognosis (Ng et al., 1995; Dohmen et al., 2003). Understanding the mechanism responsible for the higher incidence and poorer prognosis of HCC in men would also be important in tackling this devastating disease.

RESULTS

Characteristics of HCC Patients Used in This Study

We obtained snap-frozen or paraffin-embedded HCC tissues and surrounding nontumor hepatic tissues from 443 HCC patients who had undergone radical resection between 1999 and 2006. This study involved four independent cohorts of HCC patients. Cohorts 1 and 2 included 152 and 140 HCC patients, respectively, and *RIG-I* mRNA level was determined in these cohorts using a quantitative RT-PCR (qRT-PCR) assay because only RNA samples were available. The correlation of RIG-I expression with gender and survival was analyzed in these HCC cohorts. Cohorts 3 and 4 included 76 and 75 HCC patients, respectively, and they were from two independent, prospective, randomized, controlled trials of adjuvant IFN-α therapy for HCC patients (Sun et al., 2006; Lo et al., 2007; Ji et al., 2009). In cohorts 3 and 4, RIG-I protein level was determined using immunohistochemistry tissue microarray, and its correlation with gender and survival was analyzed. Furthermore, we evaluated the correlation between RIG-I expression and IFN-α therapeutic response in these patients.

Most of the HCC patients in the four cohorts were men (86.9%) and carriers of hepatitis B virus (HBV) (90.7%), had liver cirrhosis (61.4%), elevated serum α-fetoprotein (AFP) level (63.7%), and a single tumor nodule at the time of resection (78.3%) (Table 1). Clinical variables were similar in the four patient cohorts, with the exception of age, liver cirrhosis, and tumor-node-metastasis (TNM) stage. The patients in cohort 2 were relatively younger than those in the other three cohorts; fewer patients in cohort 2 and more patients in cohort 4 had liver cirrhosis, and more patients in cohort 4 had early-stage tumors. Moreover, in cohorts 3 and 4, 48.7% and 53.3% of the patients had received "intention-to-cure" adjuvant IFN-α therapy, respectively, which improved overall survival (Sun et al., 2006; Lo et al., 2007; Ji et al., 2009).

RIG-I Is the Most Significantly Decreased ISG in HCC

Because whether ISGs might modulate response to IFN-α therapy in HCC is still not well studied, we performed a cDNA microarray and focused on differentially expressed ISGs in HCC tissues, as compared to those in matched nontumor liver tissues (de Veer et al., 2001). The expression of ISGs in the four male patients examined is shown in Figure S1A available online. Among them, we found that *RIG-I* was the most significantly decreased ISG in HCC tissues (Figure S1B; Table S1). Furthermore, as compared to that in the matched nontumor liver tissues of the HCC cohorts, RIG-I expression was significantly decreased in HCC tissues of the patients in cohorts 1 and 2, respectively, as detected by qRT-PCR for its mRNA level, and in cohort 3, as detected by immunohistochemistry for its protein level (Figures 1A and 1B; Figure S1C). We conclude that RIG-I expression is significantly decreased in HCC.

We next investigated the underlying mechanism of RIG-I decrease in HCC in four HCC tissues with markedly decreased RIG-I expression (data not shown). First, we determined that

Table 1. Clinical Characteristics of HCC Patients

Variable	Cohort 1 (n = 152)	Cohort 2 (n = 140)	Cohort 3 (n = 76)	Cohort 4 (n = 75)	p Value
Gender (%)					0.277
Female	18 (11.8)	15 (10.7)	15 (19.7)	10 (13.3)	
Male	134 (88.2)	125 (89.3)	61 (80.3)	65 (86.7)	
Age (years)					<0.001
Median	48	42	52	50	
Range	20–78	23–74	24–75	30–77	
HBV (%)					0.167
Negative	19 (12.5)	7 (5.0)	8 (10.5)	7 (9.3)	
Positive	133 (87.5)	133 (95.0)	68 (89.5)	68 (90.7)	
Cirrhosis (%)					<0.001
No	40 (26.3)	88 (62.9)	37 (48.7)	6 (8.0)	
Yes	112 (73.7)	52 (37.1)	39 (51.3)	69 (92.0)	
AFP (%)					0.063
Negative, ≤20 ng/ml	65 (42.8)	40 (28.6)	31 (40.8)	25 (33.3)	
Positive, >20 ng/ml	87 (57.2)	100 (71.4)	45 (59.2)	50 (66.7)	
Tumor size (%)					0.114
≤3 cm	68 (44.7)	50 (35.7)	22 (28.9)	30 (40.0)	
>3 cm	84 (55.3)	90 (64.3)	54 (71.1)	45 (60.0)	
Tumor number (%)					0.124
=1	111 (73.0)	110 (78.6)	61 (80.3)	65 (86.7)	
>1	41 (27.0)	30 (21.4)	15 (19.7)	10 (13.3)	
TNM stage (%)					<0.001
I and II	69 (45.4)	68 (48.6)	40 (52.6)	58 (77.3)	
III and IV	83 (54.6)	72 (51.4)	36 (47.4)	17 (22.7)	

A p value < 0.05 was considered to indicate statistical significance. The p values were calculated in SPSS 17.0 using χ^2 test, except for age, which was calculated using one-way ANOVA.

the *RIG-I* gene was not very likely to be deleted in the HCC genome, as real-time PCR detected equal amounts of *RIG-I* from equal amounts of genomic DNA extracted from HCC and matched nontumor tissues (data not shown). Second, we sequenced the *RIG-I* gene including both the coding and untranslational regions from the same nontumor and HCC tissues and found no mutation (data not shown). Third, in the two CpG islands upstream of the *RIG-I*-coding region, DNA CpG was hypomethylated in both HCC and nontumor samples by using bisulfate sequencing (Figures S1D and S1E). DNA methylation inhibitor 5-azacytidine treatment also had no effect on RIG-I expression in HCC SMMC-7721 and BEL-7402 cells (data not shown). Fourth, we performed chromatin immunoprecipitation (ChIP) experiments and found that histone acetylation of the *RIG-I* gene was not significantly altered in HCC as compared to that in nontumor tissues. Histone deacetylase inhibitor trichostatin A treatment also had no effect on RIG-I expression in SMMC-7721 and BEL-7402 cells (data not shown). Fifth, as methylation of histone H3 at Lys4 (H3K4) is linked to transcriptional activation, whereas methylation of H3 at K9 or K27 and of H4 at K20 is linked to transcriptional repression (Esteller, 2008), we found that the *RIG-I* gene locus showed reduced levels of H3K4me3 but increased levels of H3K9me3 and H3K27me3 in HCC as compared to that in nontumor tissues (Figures S1F and S1G), and the level of H4K20me3 was not altered (data not shown). Taken together, these data suggest that lower RIG-I expression in HCC is at least in part mediated by deregulated histone methylation at the *RIG-I* gene locus.

Association of RIG-I Expression in HCC Tissues with HCC Progression

As RIG-I expression is significantly decreased in HCC, we further evaluated the association of RIG-I expression in HCC with the prognosis of HCC patients. Using the median value as the cutoff, we found that low RIG-I expression in HCC was significantly correlated with the reduced disease-free survival and overall survival of HCC patients in cohorts 1 and 2 and the control group patients in cohorts 3 and 4 (Figures 1C–1E). Cox proportional hazards regression analysis also determined that low RIG-I expression in the tumor is an independent predictor for reduced survival of HCC patients in the analyzed cohorts (Tables S2–S7). Thus, the dichotomized value of RIG-I expression is an independent predictor for prognosis of HCC patients. Additionally, it should be noted that the cohorts of HCC patients we analyzed were all Chinese patients with a high rate of chronic hepatitis B (90.7%). In HBV-related HCC, low RIG-I expression in HCC was also significantly correlated with poor prognosis of HCC in cohorts 1 and 2 and the control group patients in cohorts 3 and 4 (Figures 1F–1H). In HCC derived from other diseases, it was hard to analyze the data with sufficient statistical power because of the limited number of patients. Future work is needed to further confirm our conclusion in HCC patients related to other liver diseases.

Association of RIG-I Expression in Human HCC Tissue with IFN-α Therapeutic Response

Because *RIG-I* is a typical ISG, we next evaluated whether RIG-I expression in the tumor was associated with the response of patients to adjuvant IFN-α therapy. As shown in Figures 2A and 2B, IFN-α treatment provided only limited benefit to the overall survival of HCC patients in cohorts 3 and 4, whereas HCC patients with high RIG-I expression in tumors had a significant improvement in overall survival after receiving adjuvant IFN-α therapy, as compared to those in the control group. In contrast, IFN-α therapy had little effect on overall survival of HCC patients with low RIG-I expression in both cohorts. Representative images of high and low RIG-I expression in HCC tissues and the specificity of RIG-I staining in hepatocytes or HCC cells are shown in Figures S2A–S2E. Cox proportional hazards regression analysis also confirmed the enhanced effect of IFN-α treatment on survival of HCC patients in cohorts 3 and 4 who had high RIG-I expression (Table 2). In both univariate and multivariate analyses, IFN-α treatment was associated with significant improvement in overall survival of HCC patients with high RIG-I expression. A significant interaction was observed between RIG-I expression and IFN-α therapy with respect to the effect on survival ($p = 0.026$ for interaction in cohort 3; $p = 0.037$ for interaction in cohort 4). However, in patients with low RIG-I expression, IFN-α treatment had little effect on overall survival in cohorts 3 and 4 (Table S8). Thus, determination of

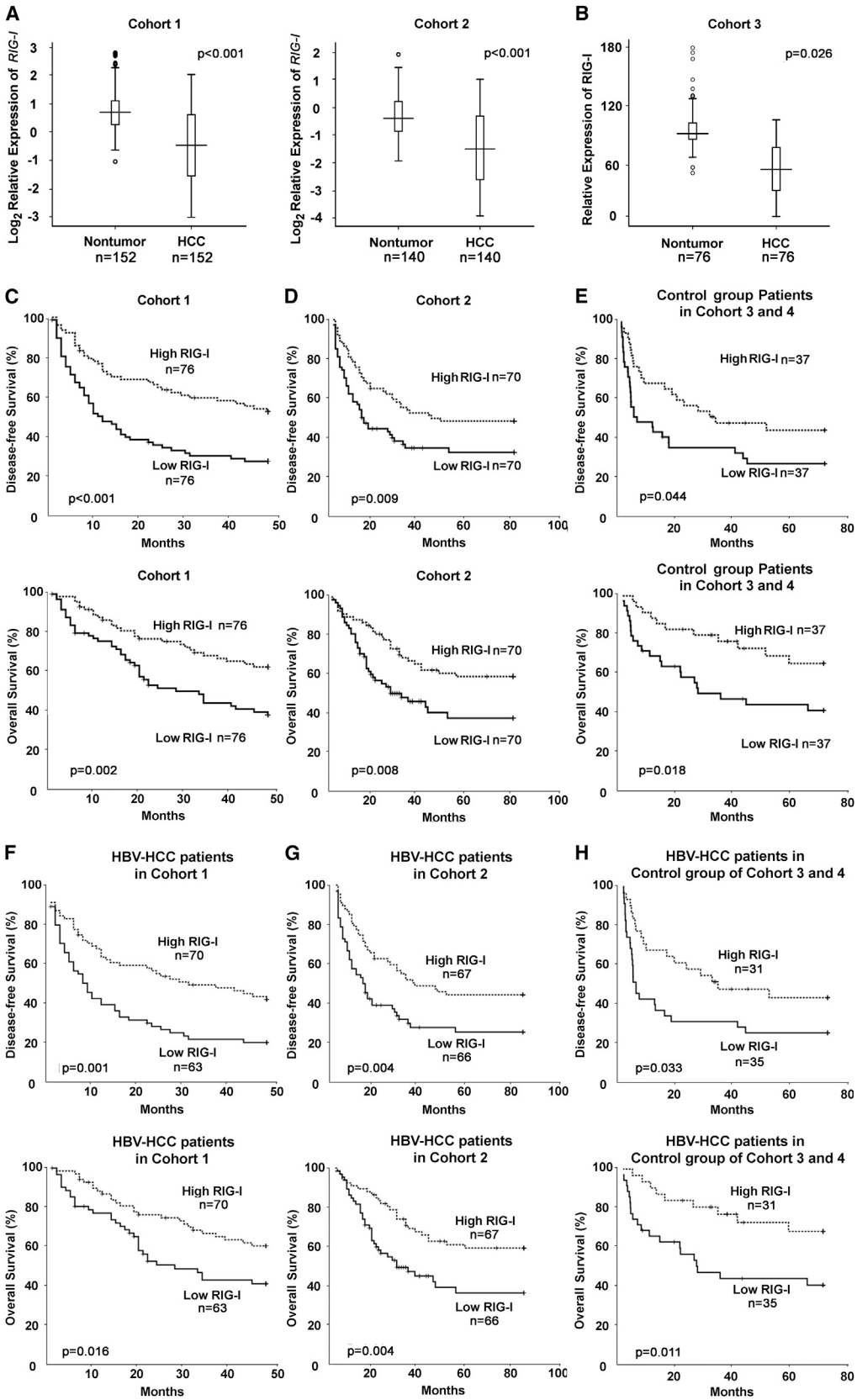

(legend on next page)

RIG-I expression in HCC tissues may be useful as an independent predictor for IFN-α treatment response.

It should be noted that these cohorts of HCC patients we analyzed were all Chinese patients with a high rate of chronic hepatitis B (Table1). In HBV-related HCC, it was also determined that only patients with high RIG-I expression in tumors had a significant improvement in overall survival after receiving adjuvant IFN-α therapy, as compared to those in the control group in both cohorts 3 and 4 (Figures 2C and 2D). In HCC derived from other diseases, it is also hard to analyze the data with enough statistical power because of the limited number of patients. The correlation between RIG-I level and IFN-α therapy responsiveness of HCC patients therefore still needs to be further evaluated in HCC patients as related to other liver diseases, although our data suggested that HBV replication seemed less relevant to RIG-I expression and IFN-α response (Figures S2F–S2H). However, these results at least suggest that determination of RIG-I expression may be useful in the prediction of IFN-α response in HBV-related HCC patients. Additionally, we also examined IFN-α receptor (IFNAR) expression in cohort 3, and found that IFNAR expression was not significantly altered in HCC tissues as compared to the matched nontumor liver tissues. IFNAR expression was also poorly correlated with IFN-α response (data not shown), thus excluding the possibility that IFN-α response of HCC patients is directly due to the altered IFNAR expression in HCC tissues. Moreover, we used the median RIG-I expression value in cohorts 3 and 4, respectively, as the cutoff point for the threshold of RIG-I expression in HCC, as median value is widely accepted in survival analyses (Ji et al., 2009). The median RIG-I staining values in cohorts 3 and 4 are 57.3 and 54.9, respectively, which are similar. We also included additional HCC tissues from 358 patients, and determined that the median RIG-I staining value is 55.9, which is also similar to those in cohorts 3 and 4. Furthermore, the median *RIG-I* mRNA expression level in HCC tissues of these 358 patients is −6.69, calculated as the cycle threshold value of β-actin minus that of RIG-I (equal to the $\log_2$ transformed value). This median value is also similar to those in cohorts 1 and 2, which are −6.75 and −6.64, respectively. Hence, this value may roughly represent the median RIG-I expression value in the HCC tissues of the patients, and IFN-α therapy may be beneficial to the HCC patients with RIG-I mRNA or protein expression higher than this value. However, although this median value is determined in a relatively larger cohort of HCC patients, this value is only a "suggested" value for IFN-α therapy. Whether this value is applicable still needs to be addressed in future large-scale prospective IFN-α therapy trials.

RIG-I Enhances Response to IFN-α Therapy in HCC

We went further to investigate the association of RIG-I expression with the response to IFN-α therapy in HCC experimental models both in vitro and in vivo. In HCC cell lines SMMC-7721 and BEL-7402, IFN-α inhibited HCC cell growth in vitro, but the inhibitory effect was reduced by *RIG-I* knockdown (Figure 3A). IFN-α-induced apoptosis of HCC cells was also suppressed by *RIG-I* knockdown (Figure 3B). These results were confirmed in the human HCC-bearing mouse model SMMC-LTNM, which was generated by transplanting histologically intact fresh human HCC tissues to form subcutaneous transplantation tumors in nude mice followed by continuous subcutaneous passaging (Hou et al., 2011). In SMMC-LTNM, the inhibitory effect of IFN-α was attenuated by intratumoral injection of cholesterol-conjugated *RIG-I* siRNA (Figures 3C and 3D), as determined by tumor size and serum AFP. Furthermore, we constructed *RIG-I* stably knocked down and *RIG-I* stably overexpressed SMMC-7721 cells and prepared HCC-bearing nude mice with different *RIG-I* expressions. The inhibitory effect of IFN-α was also significantly reduced in nude mice bearing *RIG-I* stably knocked down SMMC-7721 tumors while enhanced in *RIG-I* stably overexpressed SMMC-7721 tumors (Figures 3E–3H). Taken together, these data suggest that higher RIG-I expression in HCC enhances the antitumor effect of IFN-α.

Because the inhibitory effect of IFN-α is dependent on the induced expression of ISGs (Chawla-Sarkar et al., 2003), four ISGs associated with IFN-α-induced apoptosis were selected to evaluate the effect of RIG-I on IFN-α-induced ISG expression, including tumor necrosis factor-related apoptosis-inducing ligand (*TRAIL*), promyelocytic leukemia (*PML*), X-linked inhibitor of apoptosis protein-associated factor 1 (*XAF1*), and 2′5′A oligoadenylate synthetase 1 (*OAS1*) (Herzer et al., 2009). *RIG-I* knockdown inhibited IFN-α-induced expression of these ISGs in both HCC cell lines in vitro and SMMC-LTNM in vivo (Figures 4A and 4B). *RIG-I* deficiency also attenuated ISG induction in both hepatocytes and DEN-induced murine HCC tissues upon IFN-α stimulation (Figures 4C and 4D). Additionally, in RIG-I stably overexpressed SMMC-7721 cells, IFN-α-induced ISG expression was significantly enhanced (Figure 4E). These data demonstrate that RIG-I functionally contributes to IFN-α-induced expression of proapoptotic ISGs in HCC both in vitro and in vivo.

RIG-I Strengthens IFN-JAK-STAT Effector Signaling by Promoting STAT1 Activation through the Disruption of SHP1-STAT1 Interaction

The activation of the intracellular JAK-STAT pathway mediates the induction of ISG expression upon IFN-α stimulation (Taniguchi

Figure 1. RIG-I Expression Is Decreased in HCC, and Low RIG-I Expression Is Significantly Correlated with Poorer Prognosis of HCC Patients

(A and B) RIG-I expression in HCC and nontumor liver tissues was analyzed in cohorts 1 and 2, as determined by qRT-PCR analysis for *RIG-I* mRNA level (A), and in cohort 3, as determined by immunohistochemistry analysis for RIG-I protein level (B). The horizontal lines in the box plots represent the median, the boxes represent the interquartile range, and the whiskers represent the 2.5th and 97.5th percentiles. The p values shown were calculated using Student's t test.

(C–E) Shown are Kaplan-Meier survival curves of disease-free survival (upper) and overall survival (lower) based on dichotomized RIG-I expression in HCC tissues of cohorts 1 (C), 2 (D), and control group patients in cohorts 3 and 4 (E). The median level of RIG-I expression in each panel was used as the cutoff, with log-rank test for significance.

(F–H) Shown are Kaplan-Meier survival curves of disease-free survival (upper) and overall survival (lower) of HBV-related HCC patients in (C)–(E), with the same cutoff value and statistical analysis as in (C)–(E).

See also Figure S1 and Tables S1–S7.

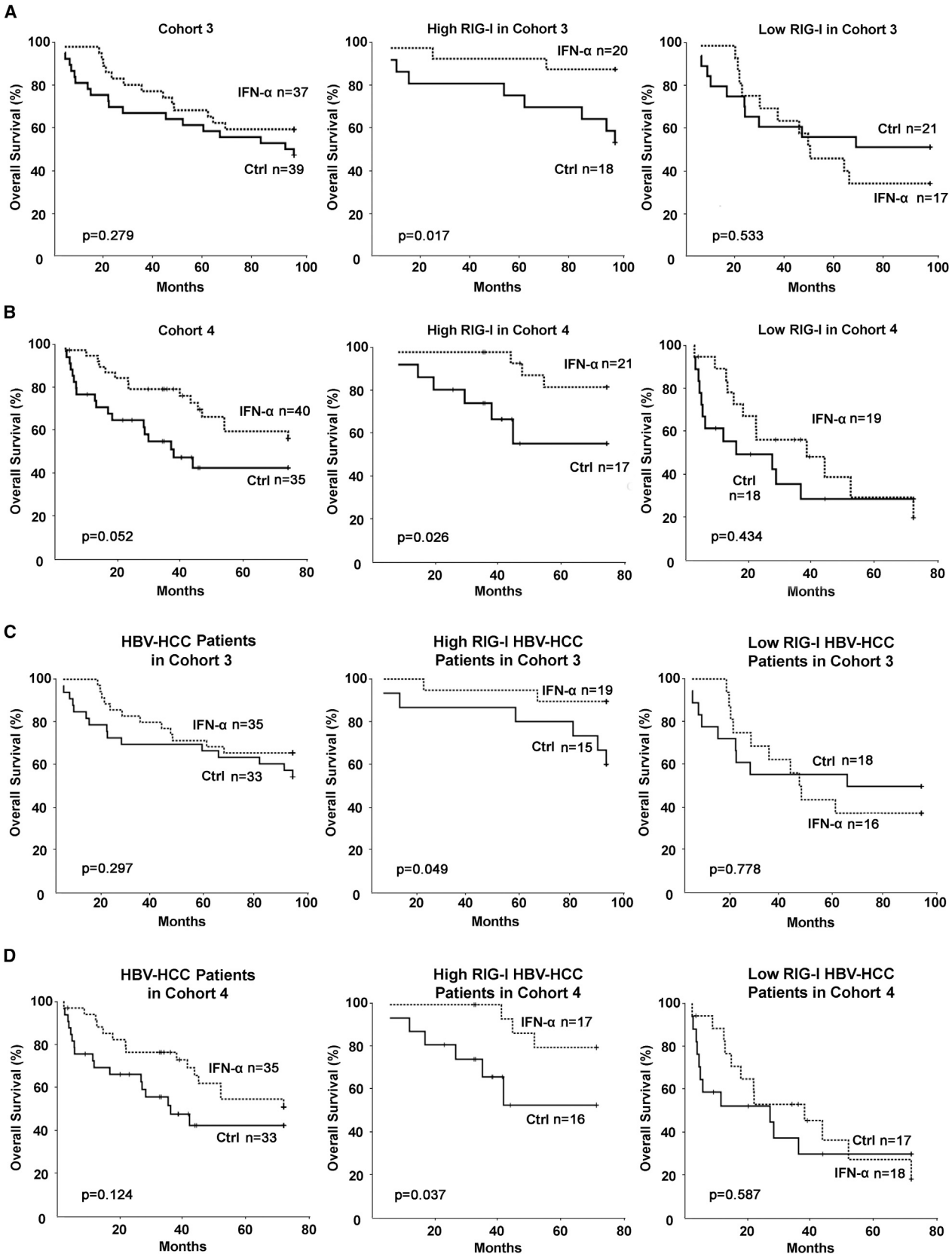

(legend on next page)

Table 2. Univariate and Multivariate Analysis of Factors Associated with Overall Survival of HCC Patients with High RIG-I Expression in Cohorts 3 and 4

	High RIG-I in Cohort 3 (n = 38)		High RIG-I in Cohort 4 (n = 38)	
Clinical Variables	Hazard Ratio (95% CI)	p Value	Hazard Ratio (95% CI)	p Value
Univariate analysis				
IFN-α versus control	0.2 (0–0.9)	0.034	0.2 (0.1–0.9)	0.040
Gender (male versus female)	2.5 (0.5–11.6)	0.256	1.0 (0.1–8.3)	0.973
Age (>50 versus ≤50 years)	31 (0.1–1510)	0.277	0.5 (0.1–1.8)	0.285
HBV (positive versus negative)	0.3 (0.1–1.6)	0.163	27 (0–5,232)	0.394
Cirrhosis (yes versus no)	2.5 (0.6–9.5)	0.194	25 (0–1,448)	0.469
AFP (≥500 versus <500 ng/ml)	0.4 (0–3.1)	0.372	0.4 (0–2.9)	0.342
Tumor size (>3 cm versus ≤3 cm)	0.9 (0.2–3.1)	0.832	1.9 (0.5–7.2)	0.327
Tumor number (>1 versus 1)	1.7 (0.8–3.4)	0.305	2.1 (0.4–10.2)	0.353
Tumor capsule (no versus yes)	2.4 (0.5–11.4)	0.262	0.7 (0.2–2.9)	0.649
Venous infiltration (yes versus no)	1.8 (0.5–6.2)	0.351	1.3 (0.3–6.1)	0.766
TNM stage (>II versus I/II)	2.8 (0.7–10.8)	0.136	1.9 (0.4–9.1)	0.430
Histological grade (>II versus I/II)	0.5 (0.1–1.7)	0.250	1.1 (0.2–5.1)	0.947
Multivariate analysis				
IFN-α versus control	0.2 (0–0.9)	0.038	0.2 (0.1–0.9)	0.036
Gender (male versus female)	1.1 (0.2–6.0)	0.941	1.9 (0.2–15.3)	0.562
TNM stage (>II versus I/II)	3.2 (0.8–13.4)	0.113	1.8 (0.4–8.8)	0.475

Analysis was conducted on HCC patients with high RIG-I expression in cohorts 3 and 4. IFN-α versus control represents 20 versus 18 patients in cohort 3 and 21 versus 17 in cohort 4. Hazard ratios (95% confidence interval; CI) and p values were calculated using univariate or multivariate Cox proportional hazards regression in SPSS 17.0. A p value < 0.05 was considered to indicate statistical significance.

and Takaoka, 2001). In HCC cells, RIG-I knockdown inhibited IFN-α-induced STAT1 activation and nuclear translocation (Figure 5A). In addition, IFN-α-induced STAT1 activation and nuclear translocation were suppressed by *RIG-I* deficiency (Figure 5B). These results suggest that RIG-I promotes the activation of IFN-JAK-STAT effector signaling in HCC cells. Furthermore, coimmunoprecipitation (co-IP) analysis revealed an inducible interaction between endogenous STAT1 with RIG-I upon IFN-α stimulation (Figure 5C). Additionally, in STAT1-silenced HCC cells, *RIG-I* knockdown did not further suppress IFN-α-induced ISG expression (Figure S3). These data suggest that RIG-I may enhance the antitumor effect of IFN-α by amplifying the IFN-JAK-STAT effector pathway in HCC cells by promoting STAT1 activation.

To identify the mechanisms responsible for RIG-I to promote STAT1 activation, we examined whether RIG-I worked as an adaptor to enhance the association of STAT1 with upstream kinases JAK1 and Tyk2. IFN-α-induced association of STAT1 with JAK1 and Tyk2 was not significantly influenced by *RIG-I* deficiency (data not shown). We next focused on the negative regulators of STAT1 and explored whether RIG-I disrupted the negative regulation of STAT1 activation. By screening the negative regulators of IFN-JAK-STAT signaling, including SHP1, SHP2, SOCS1, SOCS3, PIAS1, and PIASY (Shuai and Liu, 2003; David et al., 1995), we found that SHP1 most significantly bound STAT1 upon IFN-α stimulation in liver tissues and that SHP1-STAT1 interaction was significantly enhanced by *RIG-I* deficiency (Figure 5D; data not shown). Furthermore, in wild-type mouse liver tissue, *RIG-I* knockdown significantly suppressed IFN-α-induced TRAIL expression, whereas in *SHP1*-deficient mice, IFN-α-induced TRAIL expression was enhanced and *SHP1* deficiency abolished the *RIG-I* knockdown-mediated suppression of IFN-α-induced TRAIL expression (Figure 5E). Hence, RIG-I promotes STAT1 activation mainly through suppressing the interaction and inhibition of STAT1 by SHP1.

To identify the molecular basis responsible for RIG-I-STAT1 interaction and SHP1-STAT1 interaction, we constructed various fragments of RIG-I, SHP1, and STAT1 and found that both the CARD domain of RIG-I and the SH2 domain of SHP1 could bind the SH2-transactivation (SH2-TA) domain of STAT1, which is critical for STAT1 tyrosine phosphorylation and activation (Figures 5F and 5G). Furthermore, as SHP1 is a protein tyrosine phosphatase, we performed a biochemical in vitro dephosphorylation assay of STAT1 and found that the phosphorylated tyrosine in STAT1 could be dephosphorylated by SHP1 but that the phosphatase activity of SHP1 could be significantly inhibited by RIG-I (Figure 5H). Together, these data led us to the proposal that RIG-I may competitively bind the SH2-TA domain of STAT1 so as to disrupt the binding of STAT1 with its negative regulator SHP1. Impairment in SHP1-STAT1 interaction prevents STAT1 dephosphorylation by SHP1 and provides a basis for RIG-I-mediated promotion of STAT1 activation.

RIG-I Deficiency Promotes HCC Carcinogenesis

As RIG-I expression is determined to be significantly decreased in HCC and correlate with prognosis, we also examined whether

Figure 2. Patients with Low RIG-I Expression in HCC Have Poorer Response to IFN Therapy

(A and B) Shown is the effect of adjuvant IFN-α therapy on the overall survival of HCC patients in cohorts 3 (A) and 4 (B). Left panels show the effect in patients regardless of RIG-I expression, center panels show the effect in patients with high RIG-I expression, and right panels show the effect in patients with low RIG-I expression. The median level of RIG-I expression in each cohort was used as the cutoff (mean DAB intensity 57.3 and 54.9 in cohorts 3 and 4, respectively), with log-rank test for significance.

(C and D) Shown is the effect of adjuvant IFN-α therapy on the overall survival of HBV-related HCC patients in (A) and (B), with the same cutoff value of RIG-I expression and statistical analysis as in (A) and (B).

See also Figure S2 and Table S8.

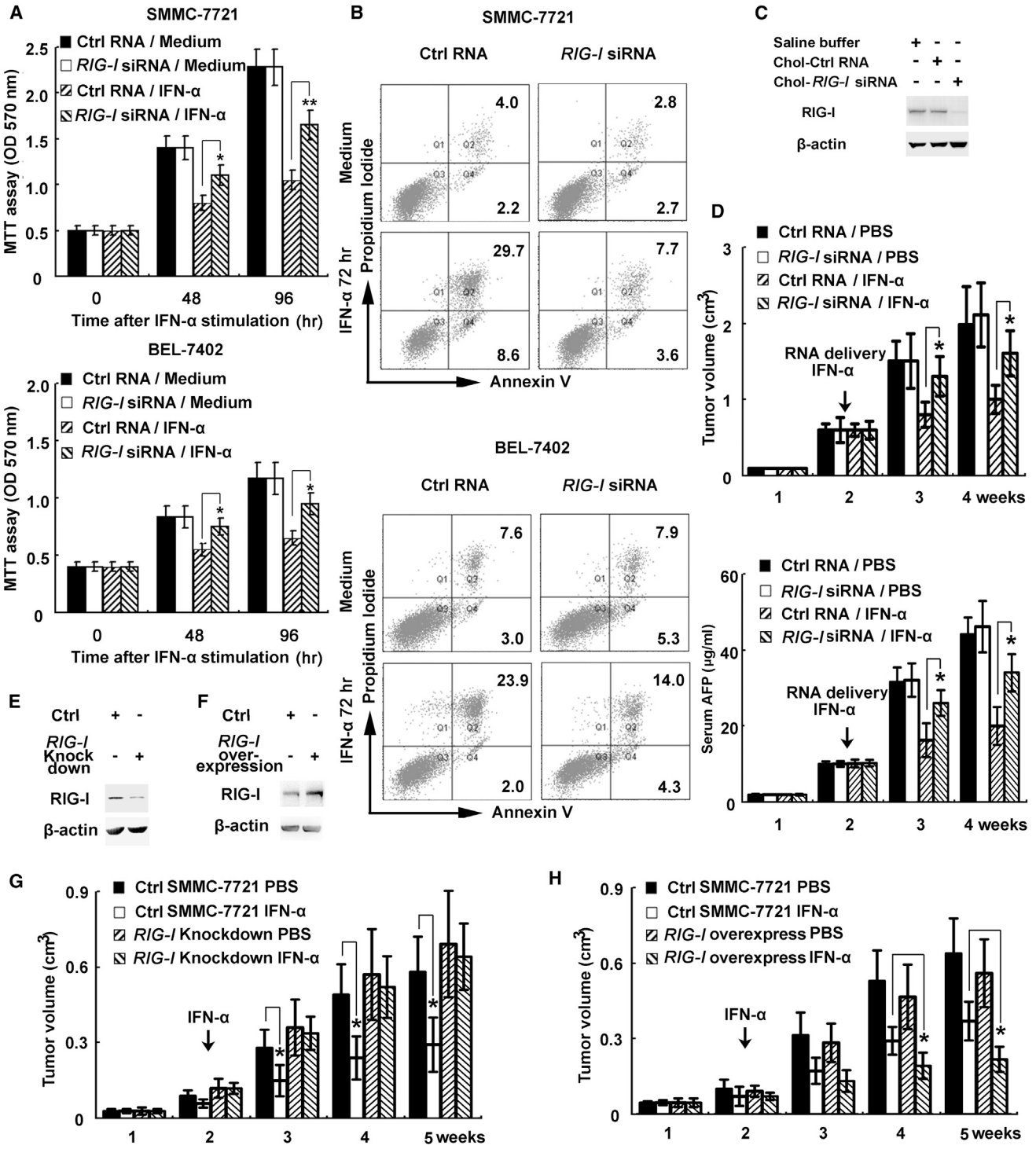

Figure 3. RIG-I Contributes to the Antitumor Effect of IFN-α Both In Vitro and In Vivo

(A) Shown is cell growth determined by MTT assay in HCC cell lines SMMC-7721 (upper) and BEL-7402 (lower) transfected with control RNA or *RIG-I* siRNA and then stimulated with 1,000 U/ml IFN-α for the indicated time.

(B) Shown is apoptosis determined by Annexin V-propidium iodide staining and flow cytometry in HCC cell lines treated as in (A).

(C) Human HCC-bearing nude mouse model SMMC-LTNM cells were intratumorally injected with saline buffer, cholesterol-conjugated control RNA, or *RIG-I* siRNA as indicated. The expression of RIG-I and β-actin (internal control) was detected by western blot.

(D) Shown are tumor growth (upper) and serum AFP (lower) in SMMC-LTNM cells administered cholesterol-conjugated control RNA or *RIG-I* siRNA and treated with IFN-α as indicated.

(legend continued on next page)

RIG-I deficiency can contribute to HCC carcinogenesis in vivo. We used the chemical carcinogen DEN-induced HCC mouse model, which mimics human HCC development, including the dependence on inflammation and gender disparity (Naugler et al., 2007; Park et al., 2010; Grivennikov et al., 2010). *RIG-I*-deficient mice used here are viable and fertile (Wang et al., 2007; Zhang et al., 2008; Hou et al., 2009). Wild-type and *RIG-I*-deficient mice were injected with a single dose of DEN on postnatal day 15, and animals were sacrificed after 8 months to examine HCC incidence (Figure 6A). *RIG-I* deficiency dramatically increased the incidence, number, and size of liver tumors (Figures 6B and 6C) and promoted HCC-related death in both male and female mice (Figure 6D). Hence, these results suggest that *RIG-I* deficiency promotes HCC carcinogenesis and that RIG-I may act as a tumor suppressor. We did not find any spontaneous tumors in aged *RIG-I*-deficient mice, and H&E staining of livers from aged *RIG-I*-deficient mice did not show any obvious spontaneous hepatitis (Figure S4A). Hepatic macrophage Kupffer cells and the produced IL-6 have been shown to play critical roles in HCC carcinogenesis (Naugler et al., 2007). However, in our experiments, we found that DEN-induced IL-6 or tumor necrosis factor α production was not significantly influenced by *RIG-I* deficiency (Figure S4B). Moreover, DEN-induced IL-6 production is still higher in *RIG-I*-deficient male mice than in females, as reported (Naugler et al., 2007), and was not reduced by *RIG-I* deficiency (Figure S4B). Thus, it is likely that *RIG-I* deficiency-promoted HCC carcinogenesis may be independent of IL-6 production and nonparenchymal cells such as Kupffer cells. However, although the potential roles of RIG-I in suppressing HCC carcinogenesis have been suggested, more investigations in the future are warranted to understand the tumor-suppressing roles of RIG-I in HCC initiation and progression.

Association of Hepatic RIG-I Expression with Gender

Because *RIG-I* deficiency promotes HCC carcinogenesis and one key feature of HCC epidemiology is gender disparity, we further investigated whether RIG-I expression might contribute to the HCC gender disparity in carcinogenesis. As shown in Figure 6E, gender disparity in HCC carcinogenesis was reduced by *RIG-I* deficiency, shown as the male versus female ratio of HCC incidence, number, and size, suggesting that RIG-I contributes to HCC gender disparity. Furthermore, we examined whether RIG-I expression in the liver was associated with gender. Because adjacent nontumor liver tissue reflects the precancerous state of human liver, we chose nontumor liver tissues to detect RIG-I expression and its association with HCC gender disparity in carcinogenesis. The clinical characteristics of the female and male HCC patients in cohorts 1, 2, and 3 were similar (Table S9). We did not perform the analysis in cohort 4 because the nontumor tissues in this cohort were not available. In cohorts 1, 2, and 3, we found that RIG-I expression in the nontumor liver tissues was significantly lower in men than in women (Figure 6F; Figure S4C). Furthermore, normal human liver tissues from 52 men and 50 women were collected, and RIG-I expression in normal human liver was also found to be significantly lower in men than in women (Figure 6G; Figures S4D and S4E). Additionally, in mouse studies, we found that RIG-I expression in normal mouse liver tissues was also significantly lower in males than in females (Figure 6H). Moreover, we found that the *RIG-I* gene locus showed an increased level of H3K4me3 but decreased H3K9me3 and H3K27me3 in normal human liver of women relative to men, and thus may contribute to the higher hepatic RIG-I expression in women than in men (Figure S4F). Taken together, our results suggest that lower hepatic RIG-I expression in men may contribute to gender disparity in HCC carcinogenesis.

DISCUSSION

It has been well accepted that RIG-I is an intracellular viral RNA sensor and that its activation can initiate host innate immune response, especially type I IFN production, to eliminate viral infection (Takeuchi and Akira, 2010; Luo et al., 2011; Kowalinski et al., 2011; Jiang et al., 2011a). However, recent investigations of RIG-I in cancer also reported that RIG-I activation by its ligand pppRNA could induce apoptosis in melanoma cells and ovarian cancer cells (Besch et al., 2009; Kübler et al., 2010), and inhibition of proliferation in acute myeloid leukemia cells could be augmented by RIG-I expression upon retinoic acid treatment (Jiang et al., 2011b). Consistent with these findings, our data also suggest that RIG-I may be a tumor suppressor in HCC. However, RIG-I expression may not be directly involved in the apoptosis of HCC cells, as *RIG-I* knockdown poorly influences the apoptosis induced by TRAIL or the chemotherapeutic drugs doxorubicin and cisplatin (data not shown). We presume that pppRNA-induced apoptosis is due to the activation of RIG-I, especially the activation of RIG-I downstream signaling. The induced RIG-I expression upon IFN-α stimulation may be a positive feedback of IFN-α response to amplify IFN-α effector signaling and ensure a longtime IFN-α efficacy, including IFN-α-induced apoptosis. Hence, both RIG-I expression and activation may have tumor-suppressive effects in cancer cells.

The IFN-JAK-STAT pathway is known to be negatively regulated by the phosphatase SHP1 (David et al., 1995; Shuai and Liu, 2003). We found that RIG-I promotes STAT1 activation through the disruption of SHP1-STAT1 interaction. Phosphorylation of the tyrosine at residue 701 located in the SH2-TA domain is well established as playing critical roles in IFN-α-induced STAT1 activation, dimerization, and transactivation of ISGs. The STAT1 SH2-TA domain and phosphorylation of tyrosine 701 are tightly regulated by multiple mechanisms to ensure proper response to IFN-α (Shuai and Liu, 2003), and RIG-I is found to bind this SH2-TA domain to prevent the dephosphorylation or negative regulation of STAT1. Although RIG-I-promoted STAT1 activation is abolished by *SHP1* deficiency, we do not exclude the possibility that RIG-I may also inhibit the interaction of STAT1 with other molecules (especially negative regulators) or that RIG-I may directly facilitate STAT1 activation. Furthermore,

(E and F) Shown is RIG-I expression in *RIG-I* stably knocked down (E) or overexpressed (F) SMMC-7721 cells.
(G and H) Shown is tumor growth of nude mice bearing *RIG-I* stably knocked down (G) or overexpressed (H) SMMC-7721 tumors treated with IFN-α as indicated. Experimental data are shown as mean ± SD (n = 4) or photographs of one representative experiment. Similar results were obtained in three independent experiments. *p < 0.05; **p < 0.01.

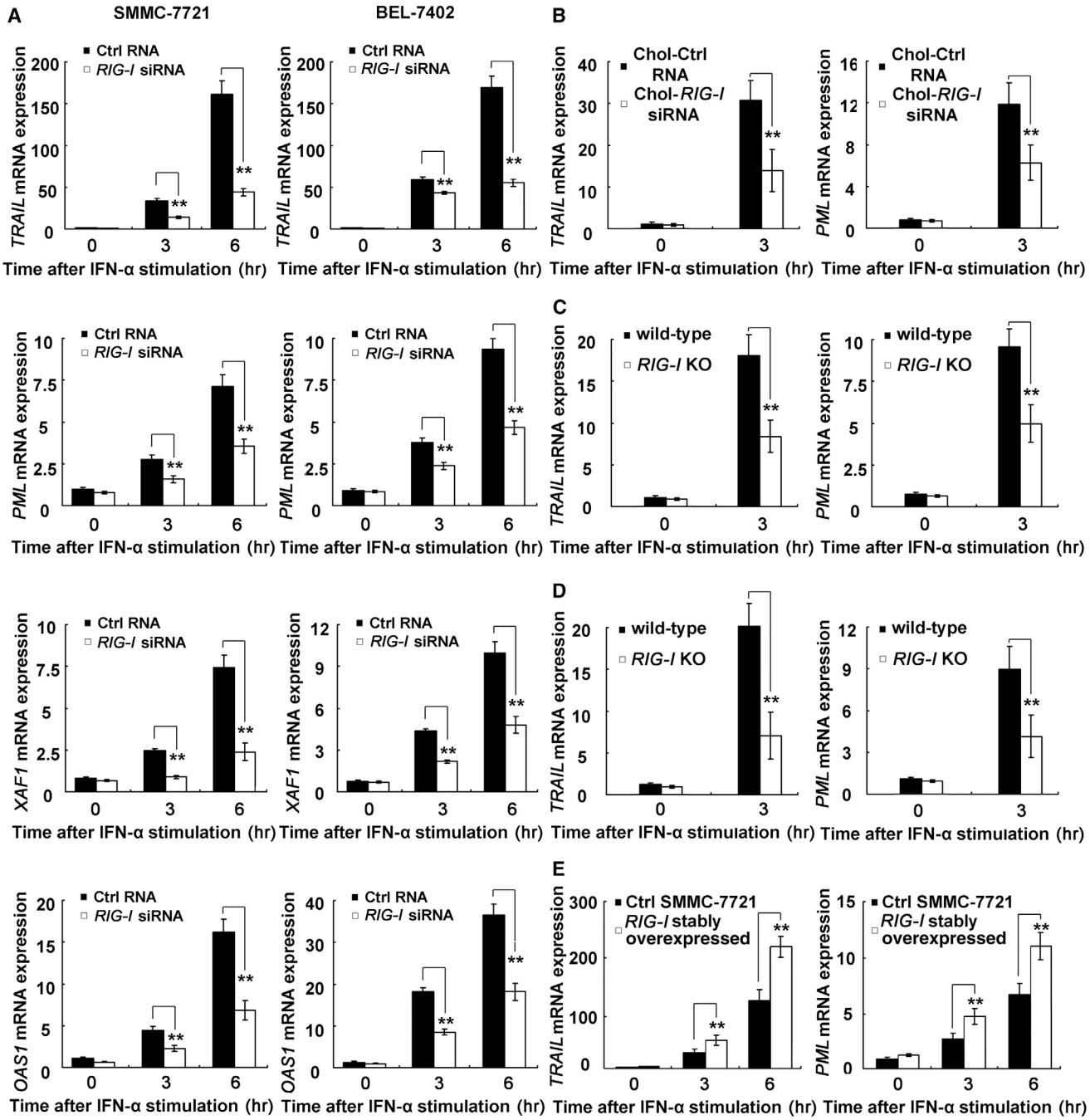

Figure 4. RIG-I Enhances IFN-α-Induced ISG Expression in HCC

(A) Shown is the induced ISG expression determined by qRT-PCR in HCC cell lines transfected with *RIG-I* siRNA and then stimulated with 1,000 U/ml IFN-α for the indicated time.

(B) Shown is the induced ISG expression in SMMC-LTNM cells administered cholesterol-conjugated *RIG-I* siRNA for 72 hr and then treated with IFN-α as indicated.

(C) Shown is the induced ISG expression in wild-type or *RIG-I*-deficient (*RIG-I* KO) hepatocytes stimulated with 1,000 U/ml recombinant mouse IFN-α as indicated.

(D) Shown is the induced ISG expression in DEN-induced HCC tissues of wild-type or *RIG-I*-deficient (*RIG-I* KO) mice followed by IFN-α stimulation.

(E) Shown is the induced ISG expression in control or *RIG-I* stably overexpressed SMMC-7721 cells stimulated with IFN-α for the indicated time.

Data are shown as mean ± SD (n = 4) of one representative experiment. Similar results were obtained in three independent experiments. **p < 0.01.

we found that the RIG-I CARD domain directly binds the SH2-TA domain of STAT1. As the CARD domain is known to activate downstream RIG-I antiviral signaling upon RIG-I activation, its interaction with STAT1 suggests that RIG-I may also function as an important intracellular regulator to modulate other signaling pathways. This hypothesis needs further testing and

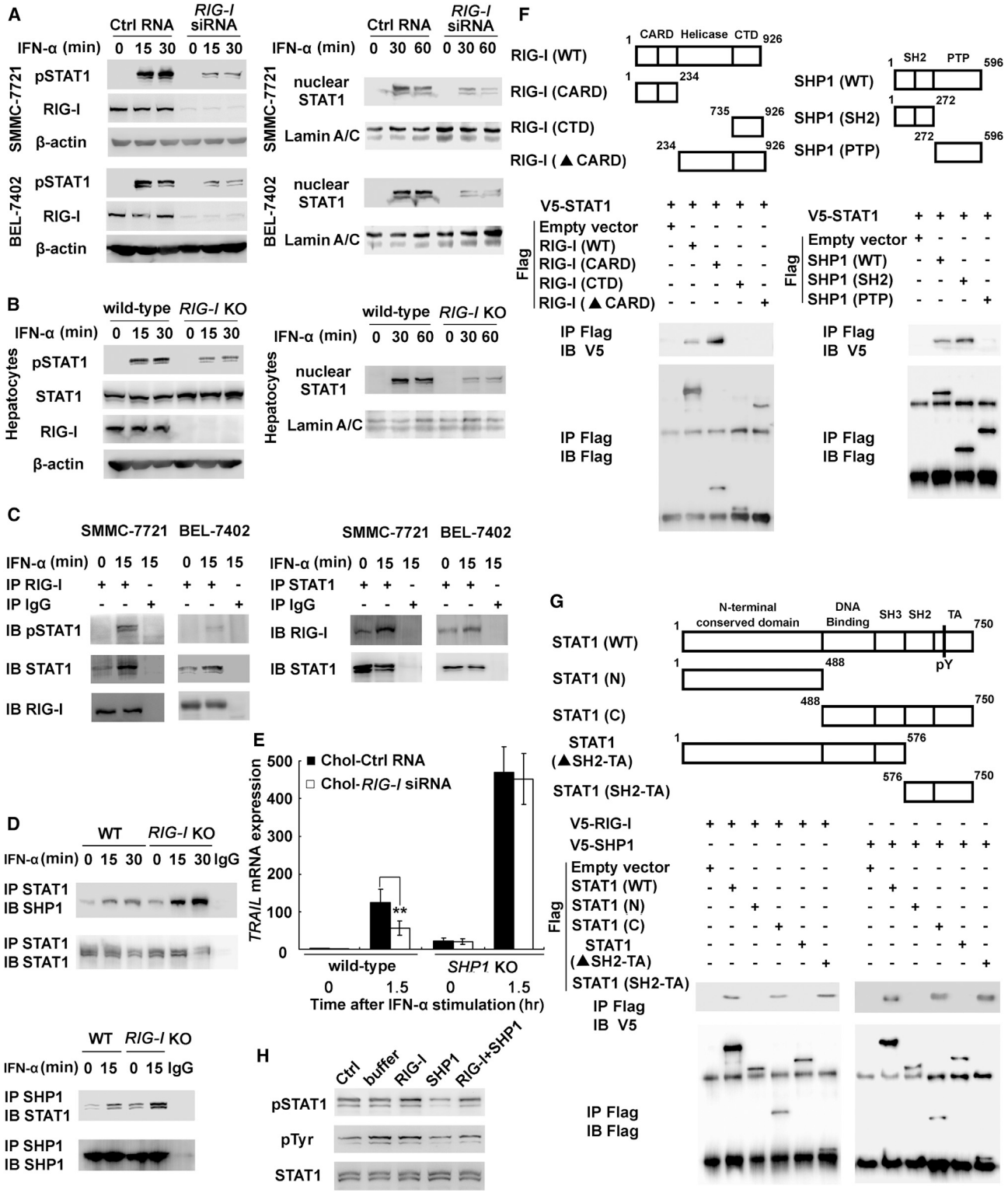

Figure 5. RIG-I Amplifies the IFN-JAK-STAT Pathway in HCC by Promoting STAT1 Activation

(A) Shown are STAT1 phosphorylation (left) and nuclear translocation (right) determined by western blot in HCC cell lines transfected with RIG-I siRNA and stimulated with IFN-α, β-actin as internal control, and Lamin A/C as nuclear marker and internal control.

(B) Shown is the confirmation of (A) determined in wild-type and *RIG-I*-deficient (*RIG-I* KO) hepatocytes.

(C) Shown is the endogenous interaction of STAT1 and RIG-I determined by co-IP in HCC cell lines. The left panel shows the detected STAT1 and phosphorylated STAT1 in the precipitates of RIG-I. The right panel shows the detected RIG-I in the precipitates of STAT1. IB, immunoblot.

(legend continued on next page)

may reveal interesting new roles of intracellular pattern-recognition receptors in the regulation of cell signaling. Moreover, it is known that RIG-I antiviral signaling induces the production of type I IFN, which activates the downstream JAK-STAT pathway to induce ISG expression (Takeuchi and Akira, 2010). Here we find that the ISG RIG-I can amplify IFN-α effector signaling. It will be interesting to study the crosstalk between the RIG-I and IFN downstream pathways, especially the regulation of IFN downstream signaling by molecules in the RIG-I pathway.

Molecular profiling and identification of diagnostic and prognostic biomarkers for HCC patients have attracted much attention (Mínguez and Lachenmayer, 2011; Budhu et al., 2006). Deregulated expression of both coding genes and noncoding RNAs in HCC has been suggested to have considerable potential in predicting the prognosis of HCC patients (Hoshida et al., 2008, 2010). We report here that RIG-I expression in HCC tissues significantly correlates with patient survival, suggesting a potential molecule with prognostic value. In combination with previous reports, simultaneous analysis of multiple genes may also prove more accurate in predicting HCC prognosis. A previous report also showed that patients with reduced miR-26 expression in HCC had a favorable response to adjuvant IFN-α therapy (Ji et al., 2009). It would be interesting to investigate whether potential correlations exist between miR-26 and RIG-I expression in HCC and whether combined detection of miR-26 and RIG-I expression may be more precise in identifying responders to IFN-α therapy.

The detailed mechanisms of RIG-I in preventing HCC carcinogenesis need to be further investigated. We postulate that host IFN-α may be important in the prevention of HCC carcinogenesis and that low expression of RIG-I may impair cellular response to IFN-α, promoting HCC carcinogenesis. Moreover, as STAT1 activation has been shown to suppress HCC development (Chen et al., 2013a; Zhu et al., 2010), the promotion of STAT1 activation by RIG-I may also have tumor-suppressive roles. There may also be other ISGs modulating IFN-α responses, and future work will be needed to fully reveal the roles of ISGs in the regulation of IFN-α effector signaling and antitumor responses.

EXPERIMENTAL PROCEDURES

Clinical Specimens

This study involved four independent cohorts of HCC patients. They were cohort 1, 152 patients from Sun Yat-sen University (Guangzhou, China); cohort 2, 140 patients from the Affiliated Tumor Hospital of Guangxi Medical University (Nanning, China); cohort 3, 76 HCC patients from the University of Hong Kong (Hong Kong, China); and cohort 4, 75 HCC patients from Zhongshan Hospital (Shanghai, China). Cohorts 3 and 4 were from two independent clinical trials of adjuvant IFN-α therapy for HCC patients. Cohort 3 included 39 HCC patients in the control group and 37 in the IFN-α-treated group, and was a subset of patients as previously reported (Lo et al., 2007). Cohort 4 included 35 HCC patients in the control group and 40 in the IFN-α-treated group, and was a subset of patients as previously reported (Sun et al., 2006). These patients had first undergone radical resection of HCC, which was made into tissue microarray slides, and then were randomly assigned to control or IFN-α-treated groups, and both groups were strictly followed as described previously (Sun et al., 2006; Lo et al., 2007). Normal human liver tissues were obtained from distal normal liver tissue of liver hemangioma patients. All samples were collected with written informed consent from the patients and were approved by the institutional review board at each study center.

Reagents

Antibodies specific to phospho-STAT1 (9171), STAT1 (9172), SHP1 (3759), β-actin (4970), and horseradish peroxidase-coupled secondary antibodies (7074 and 7076) were from Cell Signaling Technology. Antibodies specific to Lamin A/C (sc-56140) were from Santa Cruz Biotechnology. Antibodies specific to Flag tag (F1804) were from Sigma. Antibodies specific to V5 tag (ab9116) and hepatocyte-specific antigen (ab75677) were from Abcam. Cholesterol-conjugated *RIG-I* siRNA for in vivo RNA interference and its negative control were from RiboBio (Hou et al., 2011). DEN (N0258) was from Sigma.

Tissue Microarray and Immunohistochemistry

Protein levels of RIG-I expression in tissues were determined using tissue microarray (TMA). TMAs were assembled using a manual tissue puncher. The different samples were punched out from selected regions of tissues and assembled into a new paraffin block. Tissue cores were 2 mm in diameter, and the length ranged from 4 to 6 mm. TMAs were sectioned (5 μm) and stained with H&E to verify histology. The immunohistochemistry stainings were performed on 5 μm sections. The sections were placed on polylysine-coated slides, deparaffinized in xylene, rehydrated through graded ethanol, quenched for endogenous peroxidase activity in 3% hydrogen peroxide, and processed for antigen retrieval by microwave heating for 7 min in 10 mM citrate buffer (pH 6.0). The primary anti-RIG-I antibody (ab45428; Abcam) was diluted 1:200 in PBS containing 1% BSA and incubated at 4°C overnight. The next day, immunostaining was performed using the Dako ChemMate EnVision Detection Kit peroxidase/diaminobenzidine (DAB) rabbit/mouse, which resulted in a brown-colored precipitate at the antigen site. Subsequently, sections were counterstained with hematoxylin (Zymed Laboratories), mounted in nonaqueous mounting medium, and coverslipped. Pictures were acquired using a HistoFAXS system, and mean DAB staining intensity was calculated using HistoQuest software (both from TissueGnostics) (Puhr et al., 2009), which represents the quantitative protein expression level of RIG-I. In each tissue, the average DAB staining intensity of the selected two cores represents the quantitative protein expression level of RIG-I in these tissues.

In Vivo Assay

All animal experiments were undertaken in accordance with the National Institute of Health Guide for the Care and Use of Laboratory Animals, with the approval of the Scientific Investigation Board of the Second Military Medical University, Shanghai, China. All animals were housed in a virus-free facility

(D) Shown is the endogenous interaction of STAT1 and SHP1 as determined by co-IP in liver tissues of wild-type and *RIG-I*-deficient (*RIG-I* KO) mice treated by IFN-α as indicated.
(E) Wild-type or *SHP1*-deficient (*SHP1* KO) mice were injected with cholesterol-conjugated control RNA or *RIG-I* siRNA, and then TRAIL expression in liver tissues followed by peritoneal injection of 5×10^6 U/kg IFN-α was detected by qRT-PCR.
(F and G) Wild-type or fragments of RIG-I (F, left), SHP1 (F, right), and STAT1 (G) were constructed as indicated. Association of Flag-tagged RIG-I and SHP1 with V5-tagged STAT1 (F) and association of Flag-tagged STAT1 with V5-tagged RIG-I and SHP1 (G) were determined using co-IP in the transfected HEK293 cells. CTD, C-terminal domain.
(H) Shown is the in vitro dephosphorylation assay of precipitated STAT1 protein coincubated with the purified RIG-I N-terminal CARD domain, full-length SHP1, or both. Phosphorylated STAT1 and tyrosine were detected by western blot. STAT1 was detected as an input control.
Experimental data are shown as mean ± SD (n = 4) or photographs of one representative experiment. Similar results were obtained in three independent experiments. $^{**}p < 0.01$. See also Figure S3.

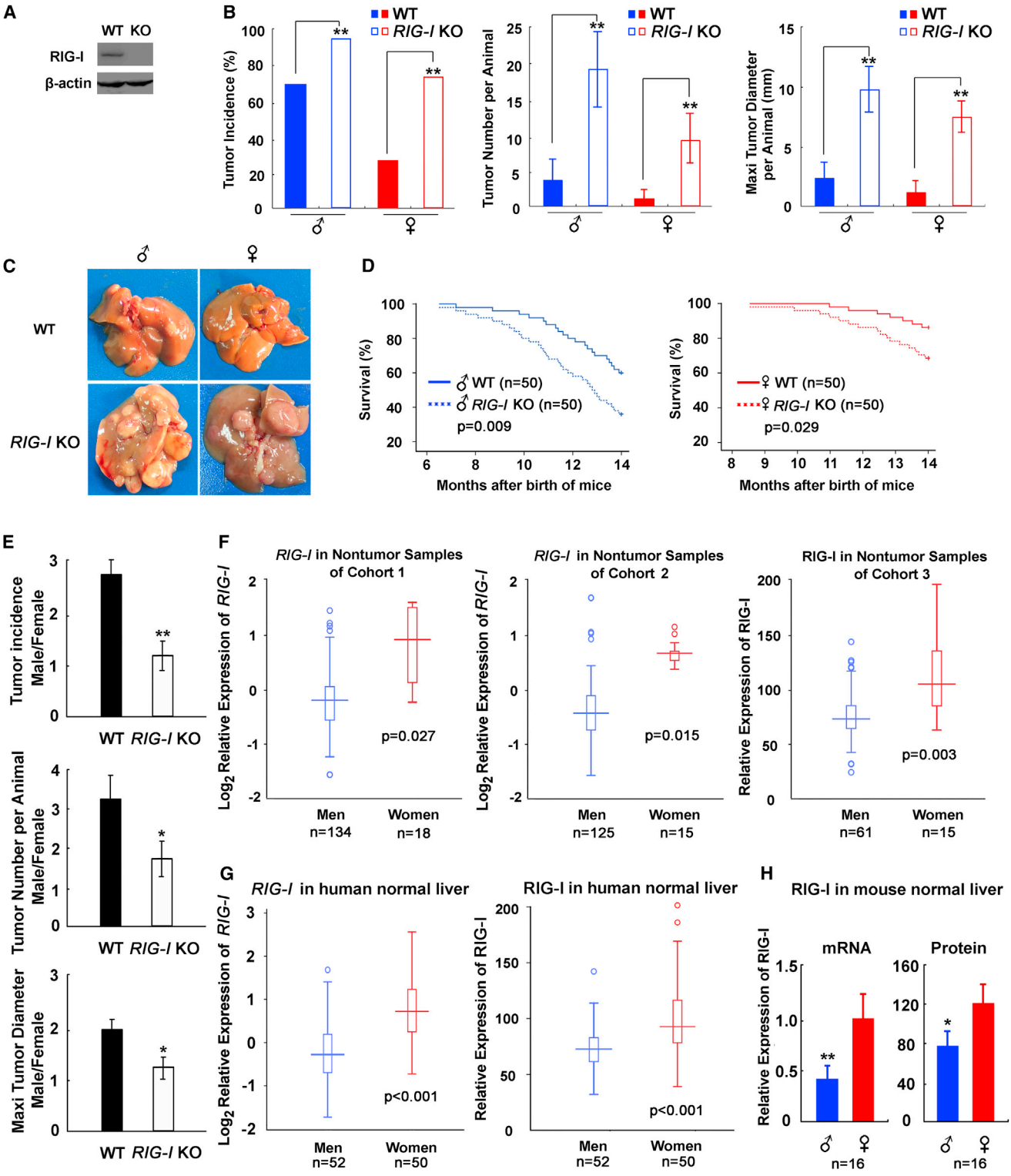

Figure 6. RIG-I Deficiency Promotes HCC Carcinogenesis and Hepatic RIG-I Expression Is Lower in Men Than in Women

(A) RIG-I expression in liver tissues of wild-type and *RIG-I*-deficient (*RIG-I* KO) mice was detected by western blot.

(B) Shown are liver tumor incidence (left; Fisher's exact test), tumor number per animal (center; unpaired t test), and maximal tumor diameter per animal (right; unpaired t test) of the DEN-induced HCC model in wild-type and *RIG-I*-deficient (*RIG-I* KO) mice. Fifty mice were included in each group. Experimental data are shown as mean ± SD (n = 50) of one representative experiment. Similar results were obtained in four independent experiments. **p < 0.01.

(C) Gross appearances of representative livers with tumors in (B).

(legend continued on next page)

and maintained in a standard temperature- and light-controlled animal facility. A human HCC-bearing nude mice model (SMMC-LTNM) was prepared by transplanting histologically intact fresh human HCC tissues to form subcutaneous transplantation tumors in nude mice and then continuously maintained with subcutaneous passage (Hou et al., 2011). For delivery of cholesterol-conjugated RNA, 10 nmol RNA in 0.1 ml saline buffer was locally injected into the tumor mass once every 3 days (Hou et al., 2011). Recombinant IFN-α-2b (5×10^6 U/kg; Kaiyinyisheng) was injected subcutaneously daily (Wang et al., 2000). Tumor size was measured and serum AFP was detected as described previously (Hou et al., 2011). For the SMMC-7721 xenograft model, 1×10^7 cells were subcutaneously injected and inoculated in nude mice and then treated with IFN-α and the effectiveness was measured. *RIG-I*-deficient mice were generated as described previously (Wang et al., 2007; Zhang et al., 2008; Hou et al., 2009). *SHP1*-deficient mice were described previously (An et al., 2008). Wild-type littermates were used as control mice. For chemical induction of hepatocarcinogenesis, mice at postnatal day 15 were injected intraperitoneally with 25 mg/kg DEN and then maintained on regular chow food as reported (Naugler et al., 2007). Livers and tumors were photographed and harvested for analysis 8 months after the initial injection. Recombinant mouse IFN-α (5×10^6 U/kg; 130-093-130; Miltenyi Biotec) was used for subcutaneous injection and stimulation.

Statistical Analysis

Data are presented as mean ± SD. Statistical comparisons between experimental groups were analyzed by unpaired Student's t test, and a two-tailed $p < 0.05$ was taken to indicate statistical significance. For analyzing the clinical variables in the HCC cohorts, χ^2 test and one-way ANOVA in SPSS 17.0 were used and the p values are indicated. Kaplan-Meier survival analysis was used to compare HCC patient survival based on dichotomized RIG-I expression using SPSS 17.0 with statistical p values generated by the log-rank test. Cox proportional hazards regression analyses were used to analyze the effect of clinical variables on patient survival using SPSS 17.0. A univariate test was used to examine the influence of each clinical variable on survival. A multivariate analysis was performed considering clinical variables from the univariate analysis that were significantly associated with survival, with significance set at $p < 0.05$. The p values and hazard ratios are indicated.

For RNA isolation and real-time qRT-PCR analysis, microarray analysis, cell lines and transfection, RNA interference, 3-(4,5-dimethylthiazol-2-yl)-2,5-diphenyltetrazolium bromide (MTT) assay, apoptosis assay, bisulfate sequencing, ChIP assay, dephosphorylation assay, confocal microscopy, tumorigenicity assay, immunoprecipitation, and western blot, please see Supplemental Experimental Procedures.

ACCESSION NUMBERS

The cDNA microarray data have been deposited in the Gene Expression Omnibus database (http://www.ncbi.nlm.nih.gov/geo) under accession number GSE34674.

SUPPLEMENTAL INFORMATION

Supplemental Information includes Supplemental Experimental Procedures, four figures, and nine tables and can be found with this article online at http://dx.doi.org/10.1016/j.ccr.2013.11.011.

ACKNOWLEDGMENTS

We thank Ms. Tingting Fang, Mei Jin, and Yan Li for technical assistance and Drs. Chaofeng Han, Xingguang Liu, Sheng Xu, Yanmei Han, Taoyong Chen, Yan Gu, and Xiaoping Su for valuable discussions. This work was supported by grants from the National 125 Key Project of China (2012ZX10002-014), National Key Basic Research Program of China (2012CB518900 and 2013CB530503), and National Natural Science Foundation of China (31170826, 31370864, 81272279, 31200585, 81102213, 81123006, and 31390431).

Received: November 6, 2012
Revised: May 13, 2013
Accepted: November 15, 2013
Published: December 19, 2013

REFERENCES

An, H., Hou, J., Zhou, J., Zhao, W., Xu, H., Zheng, Y., Yu, Y., Liu, S., and Cao, X. (2008). Phosphatase SHP-1 promotes TLR- and RIG-I-activated production of type I interferon by inhibiting the kinase IRAK1. Nat. Immunol. *9*, 542–550.

Besch, R., Poeck, H., Hohenauer, T., Senft, D., Häcker, G., Berking, C., Hornung, V., Endres, S., Ruzicka, T., Rothenfusser, S., and Hartmann, G. (2009). Proapoptotic signaling induced by RIG-I and MDA-5 results in type I interferon-independent apoptosis in human melanoma cells. J. Clin. Invest. *119*, 2399–2411.

Buch, S.C., Kondragunta, V., Branch, R.A., and Carr, B.I. (2008). Gender-based outcomes differences in unresectable hepatocellular carcinoma. Hepatol. Int. *2*, 95–101.

Budhu, A., Forgues, M., Ye, Q.H., Jia, H.L., He, P., Zanetti, K.A., Kammula, U.S., Chen, Y., Qin, L.X., Tang, Z.Y., and Wang, X.W. (2006). Prediction of venous metastases, recurrence, and prognosis in hepatocellular carcinoma based on a unique immune response signature of the liver microenvironment. Cancer Cell *10*, 99–111.

Chawla-Sarkar, M., Lindner, D.J., Liu, Y.F., Williams, B.R., Sen, G.C., Silverman, R.H., and Borden, E.C. (2003). Apoptosis and interferons: role of interferon-stimulated genes as mediators of apoptosis. Apoptosis *8*, 237–249.

Chen, G., Wang, H., Xie, S., Ma, J., and Wang, G. (2013a). STAT1 negatively regulates hepatocellular carcinoma cell proliferation. Oncol. Rep. *29*, 2303–2310.

Chen, W., Han, C., Xie, B., Hu, X., Yu, Q., Shi, L., Wang, Q., Li, D., Wang, J., Zheng, P., et al. (2013b). Induction of Siglec-G by RNA viruses inhibits the innate immune response by promoting RIG-I degradation. Cell *152*, 467–478.

Clavien, P.A. (2007). Interferon: the magic bullet to prevent hepatocellular carcinoma recurrence after resection? Ann. Surg. *245*, 843–845.

David, M., Chen, H.E., Goelz, S., Larner, A.C., and Neel, B.G. (1995). Differential regulation of the α/β interferon-stimulated Jak/Stat pathway by the SH2 domain-containing tyrosine phosphatase SHPTP1. Mol. Cell. Biol. *15*, 7050–7058.

de Veer, M.J., Holko, M., Frevel, M., Walker, E., Der, S., Paranjape, J.M., Silverman, R.H., and Williams, B.R. (2001). Functional classification of interferon-stimulated genes identified using microarrays. J. Leukoc. Biol. *69*, 912–920.

(D) The survival curves of wild-type and *RIG-I*-deficient (*RIG-I* KO) mice injected with DEN (log-rank test for significance; left, male; right, female). Experimental data are shown as Kaplan-Meier survival curves of one representative experiment, with p values shown as indicated. Similar results were obtained in four independent experiments.

(E) Shown are male versus female ratios of liver tumor incidence, tumor number per animal, and maximal tumor diameter per animal depicted in (B). Data are shown as mean ± SD (n = 4) of four independent experiments. *$p < 0.05$; **$p < 0.01$.

(F and G) Shown is RIG-I expression in nontumor liver tissues from female and male HCC patients in cohorts 1, 2, and 3 (F), as well as in human normal liver tissues of men and women (G; left, mRNA level; right, protein level). The horizontal lines in the box plots represent the median, boxes represent the interquartile range, and whiskers represent the 2.5th and 97.5th percentiles. The p values shown were calculated using Student's t test.

(H) Shown is RIG-I expression in normal liver of male and female mice as indicated. Data are shown as mean ± SD (n = 16) of one representative experiment. Similar results were obtained in three independent experiments. *$p < 0.05$; **$p < 0.01$.

See also Figure S4 and Table S9.

Dohmen, K., Shigematsu, H., Irie, K., and Ishibashi, H. (2003). Longer survival in female than male with hepatocellular carcinoma. J. Gastroenterol. Hepatol. *18*, 267–272.

El-Serag, H.B. (2011). Hepatocellular carcinoma. N. Engl. J. Med. *365*, 1118–1127.

El-Serag, H.B., and Rudolph, K.L. (2007). Hepatocellular carcinoma: epidemiology and molecular carcinogenesis. Gastroenterology *132*, 2557–2576.

Esteller, M. (2008). Epigenetics in cancer. N. Engl. J. Med. *358*, 1148–1159.

Finn, O.J. (2008). Cancer immunology. N. Engl. J. Med. *358*, 2704–2715.

Grivennikov, S.I., Greten, F.R., and Karin, M. (2010). Immunity, inflammation, and cancer. Cell *140*, 883–899.

Herzer, K., Hofmann, T.G., Teufel, A., Schimanski, C.C., Moehler, M., Kanzler, S., Schulze-Bergkamen, H., and Galle, P.R. (2009). IFN-α-induced apoptosis in hepatocellular carcinoma involves promyelocytic leukemia protein and TRAIL independently of p53. Cancer Res. *69*, 855–862.

Hoshida, Y., Villanueva, A., Kobayashi, M., Peix, J., Chiang, D.Y., Camargo, A., Gupta, S., Moore, J., Wrobel, M.J., Lerner, J., et al. (2008). Gene expression in fixed tissues and outcome in hepatocellular carcinoma. N. Engl. J. Med. *359*, 1995–2004.

Hoshida, Y., Toffanin, S., Lachenmayer, A., Villanueva, A., Minguez, B., and Llovet, J.M. (2010). Molecular classification and novel targets in hepatocellular carcinoma: recent advancements. Semin. Liver Dis. *30*, 35–51.

Hou, J., Wang, P., Lin, L., Liu, X., Ma, F., An, H., Wang, Z., and Cao, X. (2009). MicroRNA-146a feedback inhibits RIG-I-dependent type I IFN production in macrophages by targeting TRAF6, IRAK1, and IRAK2. J. Immunol. *183*, 2150–2158.

Hou, J., Lin, L., Zhou, W., Wang, Z., Ding, G., Dong, Q., Qin, L., Wu, X., Zheng, Y., Yang, Y., et al. (2011). Identification of miRNomes in human liver and hepatocellular carcinoma reveals miR-199a/b-3p as therapeutic target for hepatocellular carcinoma. Cancer Cell *19*, 232–243.

Ji, J., Shi, J., Budhu, A., Yu, Z., Forgues, M., Roessler, S., Ambs, S., Chen, Y., Meltzer, P.S., Croce, C.M., et al. (2009). MicroRNA expression, survival, and response to interferon in liver cancer. N. Engl. J. Med. *361*, 1437–1447.

Jiang, F., Ramanathan, A., Miller, M.T., Tang, G.Q., Gale, M., Jr., Patel, S.S., and Marcotrigiano, J. (2011a). Structural basis of RNA recognition and activation by innate immune receptor RIG-I. Nature *479*, 423–427.

Jiang, L.J., Zhang, N.N., Ding, F., Li, X.Y., Chen, L., Zhang, H.X., Zhang, W., Chen, S.J., Wang, Z.G., Li, J.M., et al. (2011b). RA-inducible gene-I induction augments STAT1 activation to inhibit leukemia cell proliferation. Proc. Natl. Acad. Sci. USA *108*, 1897–1902.

Kowalinski, E., Lunardi, T., McCarthy, A.A., Louber, J., Brunel, J., Grigorov, B., Gerlier, D., and Cusack, S. (2011). Structural basis for the activation of innate immune pattern-recognition receptor RIG-I by viral RNA. Cell *147*, 423–435.

Kübler, K., Gehrke, N., Riemann, S., Böhnert, V., Zillinger, T., Hartmann, E., Pölcher, M., Rudlowski, C., Kuhn, W., Hartmann, G., and Barchet, W. (2010). Targeted activation of RNA helicase retinoic acid-inducible gene-I induces proimmunogenic apoptosis of human ovarian cancer cells. Cancer Res. *70*, 5293–5304.

Llovet, J.M., Burroughs, A., and Bruix, J. (2003). Hepatocellular carcinoma. Lancet *362*, 1907–1917.

Llovet, J.M., Ricci, S., Mazzaferro, V., Hilgard, P., Gane, E., Blanc, J.F., de Oliveira, A.C., Santoro, A., Raoul, J.L., Forner, A., et al.; SHARP Investigators Study Group (2008). Sorafenib in advanced hepatocellular carcinoma. N. Engl. J. Med. *359*, 378–390.

Lo, C.M., Liu, C.L., Chan, S.C., Lam, C.M., Poon, R.T., Ng, I.O., Fan, S.T., and Wong, J. (2007). A randomized, controlled trial of postoperative adjuvant interferon therapy after resection of hepatocellular carcinoma. Ann. Surg. *245*, 831–842.

Luo, D., Ding, S.C., Vela, A., Kohlway, A., Lindenbach, B.D., and Pyle, A.M. (2011). Structural insights into RNA recognition by RIG-I. Cell *147*, 409–422.

Melief, C.J. (2008). Cancer immunotherapy by dendritic cells. Immunity *29*, 372–383.

Mínguez, B., and Lachenmayer, A. (2011). Diagnostic and prognostic molecular markers in hepatocellular carcinoma. Dis. Markers *31*, 181–190.

Naugler, W.E., Sakurai, T., Kim, S., Maeda, S., Kim, K., Elsharkawy, A.M., and Karin, M. (2007). Gender disparity in liver cancer due to sex differences in MyD88-dependent IL-6 production. Science *317*, 121–124.

Ng, I.O., Ng, M.M., Lai, E.C., and Fan, S.T. (1995). Better survival in female patients with hepatocellular carcinoma. Possible causes from a pathologic approach. Cancer *75*, 18–22.

Park, E.J., Lee, J.H., Yu, G.Y., He, G., Ali, S.R., Holzer, R.G., Osterreicher, C.H., Takahashi, H., and Karin, M. (2010). Dietary and genetic obesity promote liver inflammation and tumorigenesis by enhancing IL-6 and TNF expression. Cell *140*, 197–208.

Platanias, L.C. (2005). Mechanisms of type-I- and type-II-interferon-mediated signalling. Nat. Rev. Immunol. *5*, 375–386.

Puhr, M., Santer, F.R., Neuwirt, H., Susani, M., Nemeth, J.A., Hobisch, A., Kenner, L., and Culig, Z. (2009). Down-regulation of suppressor of cytokine signaling-3 causes prostate cancer cell death through activation of the extrinsic and intrinsic apoptosis pathways. Cancer Res. *69*, 7375–7384.

Ruggieri, A., Barbati, C., and Malorni, W. (2010). Cellular and molecular mechanisms involved in hepatocellular carcinoma gender disparity. Int. J. Cancer *127*, 499–504.

Shen, Y.C., Hsu, C., Chen, L.T., Cheng, C.C., Hu, F.C., and Cheng, A.L. (2010). Adjuvant interferon therapy after curative therapy for hepatocellular carcinoma (HCC): a meta-regression approach. J. Hepatol. *52*, 889–894.

Shuai, K., and Liu, B. (2003). Regulation of JAK-STAT signalling in the immune system. Nat. Rev. Immunol. *3*, 900–911.

Sun, H.C., Tang, Z.Y., Wang, L., Qin, L.X., Ma, Z.C., Ye, Q.H., Zhang, B.H., Qian, Y.B., Wu, Z.Q., Fan, J., et al. (2006). Postoperative interferon α treatment postponed recurrence and improved overall survival in patients after curative resection of HBV-related hepatocellular carcinoma: a randomized clinical trial. J. Cancer Res. Clin. Oncol. *132*, 458–465.

Takeuchi, O., and Akira, S. (2010). Pattern recognition receptors and inflammation. Cell *140*, 805–820.

Taniguchi, T., and Takaoka, A. (2001). A weak signal for strong responses: interferon-α/β revisited. Nat. Rev. Mol. Cell Biol. *2*, 378–386.

Vana, J., Murphy, G.P., Aronoff, B.L., and Baker, H.W. (1977). Primary liver tumors and oral contraceptives. Results of a survey. JAMA *238*, 2154–2158.

Wang, L., Tang, Z.Y., Qin, L.X., Wu, X.F., Sun, H.C., Xue, Q., and Ye, S.L. (2000). High-dose and long-term therapy with interferon-α inhibits tumor growth and recurrence in nude mice bearing human hepatocellular carcinoma xenografts with high metastatic potential. Hepatology *32*, 43–48.

Wang, Y., Zhang, H.X., Sun, Y.P., Liu, Z.X., Liu, X.S., Wang, L., Lu, S.Y., Kong, H., Liu, Q.L., Li, X.H., et al. (2007). Rig-I$^{-/-}$ mice develop colitis associated with downregulation of Gαi2. Cell Res. *17*, 858–868.

Zhang, N.N., Shen, S.H., Jiang, L.J., Zhang, W., Zhang, H.X., Sun, Y.P., Li, X.Y., Huang, Q.H., Ge, B.X., Chen, S.J., et al. (2008). RIG-I plays a critical role in negatively regulating granulocytic proliferation. Proc. Natl. Acad. Sci. USA *105*, 10553–10558.

Zhu, Z.Z., Di, J.Z., Gu, W.Y., Cong, W.M., Gawron, A., Wang, Y., Zheng, Q., Wang, A.Z., Zhu, G., Zhang, P., and Hou, L. (2010). Association of genetic polymorphisms in STAT1 gene with increased risk of hepatocellular carcinoma. Oncology *78*, 382–388.

Zou, W. (2005). Immunosuppressive networks in the tumour environment and their therapeutic relevance. Nat. Rev. Cancer *5*, 263–274.